



Gut microorganisms and their metabolites modulate the severity of acute colitis in a tryptophan metabolism-dependent manner

Ji-Hee Shin^{1,2} · Young-Kwan Lee³ · Woo-Jeong Shon¹ · Bora Kim⁴ · Che Ok Jeon⁵ · Joo-Youn Cho⁴ · Herbert C. Morse III⁶ · Eun Young Choi³ · Dong-Mi Shin^{1,7}

Received: 1 September 2019 / Accepted: 28 January 2020 / Published online: 13 February 2020
© Springer-Verlag GmbH Germany, part of Springer Nature 2020

Abstract

Purpose Growing evidence shows that nutrient metabolism affects inflammatory bowel diseases (IBD) development. Previously, we showed that deficiency of indoleamine 2,3-dioxygenase 1 (Ido1), a tryptophan-catabolizing enzyme, reduced the severity of dextran sulfate sodium (DSS)-induced colitis in mice. However, the roles played by intestinal microbiota in generating the differences in disease progression between *Ido1*^{+/+} and *Ido1*^{-/-} mice are unknown. Therefore, we aimed to investigate the interactions between the intestinal microbiome and host IDO1 in governing intestinal inflammatory responses.

Methods Microbial 16s rRNA sequencing was conducted in *Ido1*^{+/+} and *Ido1*^{-/-} mice after DSS treatment. Bacteria-derived tryptophan metabolites were measured in urine. Transcriptome analysis revealed the effects of the metabolite and IDO1 expression in HCT116 cells. Colitis severity of *Ido1*^{+/+} was compared to *Ido1*^{-/-} mice following fecal microbiota transplantation (FMT).

Results Microbiome analysis through 16S-rRNA gene sequencing showed that IDO1 deficiency increased intestinal bacteria that use tryptophan preferentially to produce indolic compounds. Urinary excretion of 3-indoxyl sulfate, a metabolized form of gut bacteria-derived indole, was significantly higher in *Ido1*^{-/-} than in *Ido1*^{+/+} mice. Transcriptome analysis showed that tight junction transcripts were significantly increased by indole treatment in HCT116 cells; however, the effects were diminished by IDO1 overexpression. Using FMT experiments, we demonstrated that bacteria from *Ido1*^{-/-} mice could directly attenuate the severity of DSS-induced colitis.

Conclusions Our results provide evidence that a genetic defect in utilizing tryptophan affects intestinal microbiota profiles, altering microbial metabolites, and colitis development. This suggests that the host and intestinal microbiota communicate through shared nutrient metabolic networks.

Keywords Gut microbiota · Indoleamine 2,3-dioxygenase 1 · Colitis · Indole · Tryptophan

Electronic supplementary material The online version of this article (<https://doi.org/10.1007/s00394-020-02194-4>) contains supplementary material, which is available to authorized users.

✉ Eun Young Choi
eycii@snu.ac.kr

✉ Dong-Mi Shin
shindm@snu.ac.kr

¹ Department of Food and Nutrition, Seoul National University College of Human Ecology, Seoul 08826, Korea

² Research Group of Healthcare, Research Division of Food Functionality, Korea Food Research Institute, Wanju-gun 55365, Republic of Korea

³ Department of Biomedical Sciences, Graduate School of Seoul National University, Seoul 03080, Republic of Korea

⁴ Department of Clinical Pharmacology and Therapeutics, Seoul National University College of Medicine and Hospital, Seoul 03080, Republic of Korea

⁵ Department of Life Science, Chung-Ang University, 84 Huekseok-ro, Dongjak-gu, Seoul 06974, Republic of Korea

⁶ Virology and Cellular Immunology Section, Laboratory of Immunogenetics, National Institutes of Allergy and Infectious Diseases, National Institutes of Health, Rockville, MD 20852, USA

⁷ Research Institution of Human Ecology, Seoul National University, Seoul 08826, Republic of Korea

Introduction

The gastrointestinal tract contains a vast population of commensal bacteria, known as the gut microbiota. Gut microbiota are referred to as "the forgotten organ," showing similarity to organs in terms of their biological function and complexity [1]. If the balance of gut microbiota is disturbed, dysbiosis of the microbiome causes intestinal diseases such as inflammatory bowel diseases (IBD) [2]. Over the past decade, the bidirectional relationship between the gut microbiota and IBD has been one of the most-studied aspects of IBD pathogenesis.

The gut microbiota can be affected by environmental factors such as diet [3], lifestyle [4], and geographic location [5]. Previous studies have reported that geographical differences, both across different countries [6, 7] and within the same country [5, 8], contribute to shaping the human gut microbiota. The differences are closely related to variability in dietary habits or dietary products, which are influenced by the geographical provenance of individuals [9]. In addition to human studies, it has recently been shown that genetically similar murine models can show extensive gut microbial variation depending on their housing conditions, for example, specific pathogen-free (SPF) and conventional conditions [10, 11].

Tryptophan, an essential amino acid, has a therapeutic effect in dextran sulfate sodium (DSS)-induced colitis by decreasing the expression of pro-inflammatory cytokines [12, 13]. Tryptophan is metabolized by indoleamine 2,3-dioxygenase 1 (IDO1), the first and rate-limiting enzyme, as well as IDO2 and tryptophan-2, 3-dioxygenase. In particular, *IDO1* is highly expressed in colonic tissues, and is highly expressed in patients with ulcerative colitis and Crohn's disease [14]. A previous study in our laboratory showed that *Ido1*-knockout mice had less severe colitis than wild-type mice [15]. However, despite the importance of commensal bacteria in the development of colitis, the role IDO1 plays in colitis from the perspective of gut microbiota remains unclear.

The present study evaluated the roles of *Ido1* in modulating the profiles of intestinal microbiota, and identified bacterial taxa that ameliorate the severity of experimental colitis in *Ido1*-deficient mice. 16S rRNA gene sequencing approaches were used to analyze the gut microbiome in mice and the effects of bacterial metabolites on the transcriptome of colon cells. Fecal microbiota transplantation (FMT) from *Ido1*^{-/-} mice or *Ido1*^{+/+} mice to *Ido1*^{-/-} mice or *Ido1*^{+/+} mice was performed to examine the effect of microbial reconstitution on disease development.

Methods

Animal

Ido1 knockout (*Ido1*^{-/-}) mice with the C57BL/6J genetic background were purchased from Jackson Laboratory (Bar Harbor, Maine, USA) [15]. *Ido1*^{-/-} mice were crossed with C57BL/6J wild-type mice to generate the *Ido1*^{-/-} and *Ido1*^{+/+} offspring used in this study. Mice were female, 10–12 weeks old, and weighed 18–23 g. Age- and weight-matched female littermates were used as controls. All mice were fed a standard rodent diet (Purina Laboratory rodent chow diet 38057; Purina Korea Inc., Seoul, Korea) ad libitum. Mice were kept in different cages under conditions of a SPF animal facility at the Biomedical Center for Animal Resource Development (BCARD) of Seoul National University College of Medicine (Seoul, Korea). All experimental protocols were approved by the Institutional Animal Care and Use Committee of the Institute of Laboratory Animal Resources, Seoul National University (Institutional Animal Care and Use Committee permit number: SNU-150119-5).

Induction and evaluation of DSS-induced acute colitis

As previously described [15], *Ido1*^{-/-} and *Ido1*^{+/+} mice were treated with two different concentrations of DSS (MW 36,000–50,000, MP Biomedicals, Illkirch, France) (1% and 2%) in drinking water for 7 days ad libitum, and control mice received drinking water without DSS ($n=4-8$ per group). The subsequent course of colitis development was evaluated daily by scoring via the disease activity index (DAI). The DAI score was calculated by grading on a 0–4 scale based on the following parameters: change in bodyweight (1, 5–10%; 2, 11–15%; 3, 16–20%; and 4, $\geq 21\%$), stool consistency (0, normal; 2, loose stools; 4, diarrhea), and stool blood (0, no blood seen; 2, obvious blood with stool; 4, grossly bloody stool). Seven days after DSS-colitis induction, mice were euthanized with excess CO₂ gas. Food was removed from mice the night before sacrifice. After sacrifice, the proximal to distal colon was quickly removed, and colonic contents were collected by gently scraping the colonic mucosa. The colonic contents were frozen in liquid nitrogen and stored at -80°C until analysis.

Bacterial 16S rRNA gene pyrosequencing and analysis

An average of 110 mg intestinal contents were homogenized in ASL buffer using an IKA[®] T-10 Basic Ultra-Turrax homogenizer (IKA Werke GmbH & Co., Staufen,

Germany) at power level 5.5 for 1 min. Then, the suspension was heated at an optional high-temperature step (95 °C) to lyse gram-positive bacterial cells. In the last incubation step, we increased the time from 1 to 5 min to increase DNA yield. Hypervariable regions (V1–V3) of the 16S rRNA gene were amplified using barcoded universal primers for each sample (Supplementary Table S1). Polymerase chain reaction (PCR) was carried out in a final volume of 50 µL, which comprised about 10 ng DNA template, 5 µL 10× Taq buffer (20 mM Mg²⁺), 1 µL 10 mM dNTP mix, 2 µL forward and reverse barcoded primers (20 pmol/µL), and 2.5 U of Taq DNA polymerase (Sol-Gent Co., Seoul, Korea). PCR reactions were run as follows: 5 min at 94 °C, followed by 30 cycles of denaturation (30 s, 94 °C), annealing (30 s, 55 °C), and extension (30 s, 72 °C); with a final extension step of 7 min at 72 °C followed by holding at 4 °C. The PCR product was confirmed using 1% agarose gel electrophoresis and visualized using a Gel Doc system (BioRad, Hercules, CA, USA). The amplified products were purified using a QIAquick PCR purification kit (Qiagen, Valencia, CA, USA), and equimolar concentrations of each amplicon from different samples were pooled and used as template for pyrosequencing. Pyrosequencing was conducted by ChunLab Inc. (Seoul, South Korea) using a 454 GS junior platform (Roche, Mannheim, Germany), according to the manufacturer's instructions.

The change in microbial community composition was determined using Ribosomal Database Project (RDP) pyrosequencing pipeline (<https://pyro.cme.msu.edu/>; release 11) [16] at each phylogenetic level. Primer sequence, key tag, and the sequences of low quality (average score < 20) were removed using the initial processing step of the RDP. Any reads containing more than one 'N' (ambiguous nucleotides), and/or reads shorter than 300 bp were excluded from further analysis. Chimeric sequences were excluded by UCHIME [17], and included in USEARCH ver. 6.0 and aligned. Chimera removed sequences were rarefied at 4200 reads per sample and classified using the RDP-classifier [18] in the RDP pipeline at a confidence threshold of 97%. Gut microbiota sequencing datasets are available in the Sequence Read Archive database (<https://www.ncbi.nlm.nih.gov/sra>, project number: PRJNA327010).

Plasmid DNA

The Human *IDO1* (*hIDO1*)-coding region tagged with Flag was subcloned into bicistronic vectors that included the internal ribosomal entry site. Enhanced green fluorescent protein (eGFP) was included as a reporter gene [19].

Cell culture and construction of *hIDO1*-expressing HCT116 stable cell lines

HCT116 colon cancer cells were obtained from Korea Cell Line Bank (KCLB, Seoul, Republic of Korea). HCT116 cells were maintained in Dulbecco's modified Eagle's medium (Gibco, Grand Island, NY, USA) supplemented with 10% bovine calf serum, penicillin, streptomycin, and gentamycin. HCT116 cells were transfected with 2 µg of the *hIDO1* recombinant DNA constructs using polyethylenimine (Sigma-Aldrich, St Louis, MO, USA) transfection reagent to generate *hIDO1*-expressing HCT116 stable cell lines. Transfected HCT116 cells were sorted on a FACS Aria (BD Bioscience, Franklin Lakes, NJ, USA) to isolate the GFP-positive *hIDO1*-expressing cells. Cells were exposed to 1 mM indole (Acros Organics, Geel, Belgium) or *N,N*-dimethylformamide (DMF) for 24 h. Then, total RNA was isolated from cells using an RNAqueous-4PCR kit (Ambion, Austin, TX, USA) following the manufacturer's instruction.

Total RNA extraction and amplicon-sequencing

RNA samples were quantified using a NanoDrop (ND-2000, Carlsbad, CA, USA) and were converted into cDNA using a MessageSensor™ RT Kit (Ambion, Austin TX, USA). RNA samples were quantified using a Qubit® RNA HS Assay Kit (Life Technologies, Carlsbad, CA, USA) and the percentage of RNA fragments larger than 200 nt was determined by smear analysis using an Agilent 2100 Bioanalyzer (Agilent Technologies, Palo Alto, CA, USA). An Ion AmpliSeq™ Transcriptome library was constructed with using an Ion Transcriptome Human Gene Expression Kit (Life Technologies, Part # MAN0010742 Rev. A.0) as per the manufacturer's protocol. Ten-nanograms of total RNA were reverse transcribed to make cDNA by random priming. The cDNA product was amplified for target genes using the Ion AmpliSeq™ Human Gene Expression Core Panel with the Ion AmpliSeq™ Library Kit Plus (PCR 16 cycle). After primer digestion, adapters and molecular barcodes were ligated to the amplicons, before magnetic bead purification. This library was amplified for a total of 5 cycles and purified. Amplicon size and DNA concentration were measured using an Agilent High Sensitivity DNA Kit (Agilent Technologies), according to the manufacturer's recommendation. Sample emulsion PCR, emulsion breaking, and enrichment were performed using the Ion PI™ Template OT2 200 Kit v3 (Life Technologies, Part #4488318 Rev. B.0), according to the manufacturer's instructions.

Multiple barcoded libraries were combined with equal molar ratios for one Ion PI™ v2 chip. Four pooled Ion AmpliSeq™ Transcriptome libraries were loaded onto a single Ion PI™ v2 chip. Subsequent emulsion PCR, and enrichment of the sequencing beads of the pooled libraries was

performed using the Ion OneTouch™ system (Life Technologies) according to the manufacturer's protocol within about 7 h. Finally, 520 Flows sequencing was done on the Ion PI™ v2 chip using an Ion PI™ Sequencing 200 Kit v3 (Life Technologies, Part #4488315 Rev. B.0) on the Ion Proton™ sequencer (Life Technologies) [20, 21]. Transcriptome sequencing datasets are available in the Gene Expression Omnibus repository (www.ncbi.nlm.nih.gov/geo/, accession number GSE83939).

Microarray analysis of small intestines and colons of mice maintained in SPF or conventional facilities

NFS.V+ mice, inbred sublines of NFS/N mice of Swiss origin [22], were maintained in the SPF or conventional animal facility in the National Institute of Health. Total RNA purified from the small intestines and colons of each 8-month-old mouse were subjected to Agilent NIAID-customized mouse gene expression arrays. Scanned images were analyzed as detailed previously [15]. Raw data were normalized using the LIMMA package in R. Differentially expressed genes (DEGs) were identified with one-way analysis of variance (ANOVA) analysis with 5% FDR. Principal component analysis (PCA) and functional classification analysis were carried out.

Determination of the level of 3-indoxyl sulfate

After DSS treatment, urine samples were collected from mice over 24 h in a metabolic cage (Jeungdo Bio & Plant Co., Seoul, Republic of Korea) before being sacrificed. Urine samples were centrifuged at 14,000 rpm for 20 min at 4 °C to remove any solid debris, and the supernatant was diluted with distilled water. A 4 µL aliquot of prepared urine sample was injected into a 2.1 × 100 mm ACQUITY 1.8 µm HSS T3 column using an ACQUITY UPLC system (Waters Corp, Milford, MA, USA) coupled to a Waters Xevo Q-TOF mass spectrometer (Waters Corp.). The urinary 3-indoxyl sulfate was identified by comparing the ms/ms fragmentation pattern of the authentic 3-indoxyl sulfate (Sigma-Aldrich). To determine the relative level of 3-indoxyl sulfate, the peak intensity of 3-indoxyl sulfate was analyzed using MarkerLynx software (Waters Corp.)

Antibiotic cocktail (ABX) treatment and fecal microbiota transplantation

Five-week-old mice were treated with ampicillin sodium salt (1 g/L; Amresco), neomycin sulfate (1 g/L; Fisher BioReagents), metronidazole (1 g/L; Sigma-Aldrich), and vancomycin hydrochloride (500 mg/L; Cayman Chemical) ad libitum for 4 weeks in their drinking water [23]. Artificial sweetener (5 g/L; Equal® Sweetener, Chicago, IL, Merisant Co.) was

added to water to enhance palatability [24]. The ABX was exchanged every other day, and replaced with normal water two days before FMT. Depletion of gut microbiota after the ABX treatment was successfully validated as described previously [25]. Fecal pellets of donor mice were homogenized in sterile phosphate-buffered saline (PBS) to 100 mg fecal pellet/1 mL of PBS. Supernatants of homogenized samples were transplanted to recipient mice by oral gavage for two consecutive days.

Statistical analysis

Quantitative results were expressed as means ± SEM. Statistical analysis was performed using one-way ANOVA followed by Bonferroni's multiple comparison procedure. Differences between the two groups were tested with an unpaired *t* test. Correlation between severity of colitis and relative abundance of genus was carried out using Spearman's correlation test. All data were analyzed using GraphPad Prism v. 6.0 (GraphPad Software, Inc., San Diego, CA, USA). We used the linear discriminant analysis (LDA) effect size (LefSe) analytical method via the Galaxy workflow framework (<https://huttenhower.sph.harvard.edu/galaxy/root>) to identify differentially abundant bacterial genera between two groups [26].

Results

Gut transcriptome profiling analysis identified tryptophan metabolism as a responder to different housing environments

To examine roles of gut microbiota in eliciting physiological responses from the host to different housing environments, we performed gene expression profiling analysis of gut tissues from mice in a SPF and compared them to those from a conventional facility (CONV). PCA identified a dramatic distinction in the gene expression patterns between CONV and SPF mice, in addition to the established tissue-specific differences between the small and large intestine (Fig. 1a). DEGs between SPF and CONV mice were classified based upon their biological functions, and the significance of each biological category was tested by Fisher's exact test. Surprisingly, amino acid metabolism was identified as one of the top five significantly modulated functions ($p < 0.001$), together with cell proliferation, gene expression, antigen presentation, and inflammatory response (Fig. 1b). Among the significant genes in the category, *Ido1* was the most highly expressed gene between CONV and SPF mice (Fig. 1c). Considering that SPF mice have dramatic differences in the gut microbiome compared to CONV mice [11], our results suggest that the difference in gut bacterial communities driven by

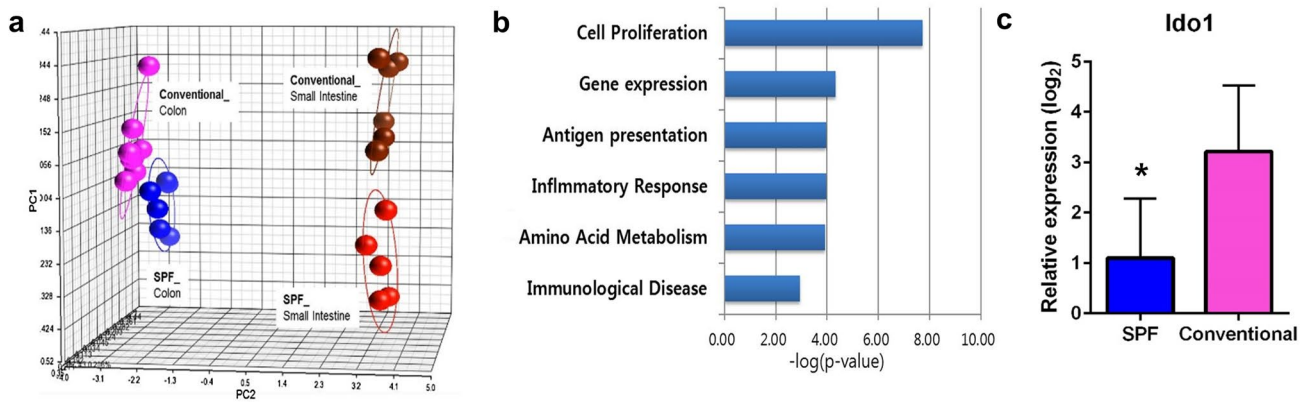


Fig. 1 Gene expression profiling analysis of intestinal tissues from mice housed in SPF or conventional facilities. Transcriptomes of small intestines and colons from mice raised in conventional ($n=6$) or SPF ($n=8$) facilities were analyzed using whole mouse genome expression microarray. **a** Principal component analysis (PCA) of DEGs. Significant genes were identified by one-way ANOVA ($p < 0.01$). Each ball represents each transcriptome of the individual

different housing conditions might have a significant impact on *Ido1* expression, and that changes in tryptophan metabolism may be one of the mediating processes between commensal intestinal bacteria and host physiological response.

Absence of *Ido1* in mice induces changes in the gut bacterial communities

The observation that different housing conditions changed the *Ido1* expression in the host, prompted us to examine if a challenge in *Ido1* expression might cause an alteration in the gut bacteria communities. To test this hypothesis, we compared the gut microbial communities from *Ido1*-deficient (*Ido1*^{-/-}) and wild-type (*Ido1*^{+/+}) mice through 16S rRNA gene sequencing analysis. In addition, we analyzed the gut microbiome of DSS-treated mice for both genotypes to characterize the changes in the inflamed tissues. To establish a murine model of colitis, *Ido1*-deficient (*Ido1*^{-/-}) and wild-type (*Ido1*^{+/+}) mice were administered either 1% or 2% DSS in drinking water. We have previously shown that clinical signs of DSS-induced colitis were less severe in *Ido1*^{-/-} mice than in *Ido1*^{+/+} mice [15]. Briefly, after DSS exposure, DAI and body weight loss were significantly elevated in *Ido1*^{+/+} mice as compared with *Ido1*^{-/-} mice [15]. When comparing colon length between *Ido1*^{+/+} mice and *Ido1*^{-/-} mice, *Ido1*^{+/+} mice showed significantly shorter colons compared to the *Ido1*^{-/-} mice after DSS exposure [15]. Additionally, histological scores of the colon in *Ido1*^{-/-} mice were significantly decreased as compared with *Ido1*^{+/+} mice [15]. These differences of clinical symptoms were not detected in 1% DSS treatment group but in 2% DSS treatment groups. Then, we compared the gut microbiota composition between

mouse. **b** Functional classification of the significant genes. Enrichment of significant genes in each category was tested by Fisher's exact test. **c** The transcript levels of *Ido1* in the colonic tissues. The relative expressions of *Ido1* are shown in \log_2 transformation. The significance in the difference between SPF vs. CONV was tested by the unpaired *t* test ($*p < 0.01$)

Ido1^{+/+} and *Ido1*^{-/-} mice by performing 16S rRNA gene sequencing. Rarefaction curves for each sample reached a plateau, proving that the depth of sequencing could describe the microbial communities reasonably well (Supplementary Fig. S1a). PCA analysis showed that the bacterial communities of *Ido1*^{-/-} mice were distinguished from those of *Ido1*^{+/+} mice, especially in the high dose (2%) DSS treatment group. Additionally, the microbiome profile in the 2% DSS-induced colitis model was clearly different from the microbiome profile in the 1% DSS model (Supplementary Fig. S1b). This result is in agreement with our previous finding that *Ido1*^{-/-} mice showed significant differences in severity of acute colitis compared to *Ido1*^{+/+} mice in the 2% DSS treatment groups [15].

To identify the specific gut bacterial taxa associated with *Ido1* genes in the host, we compared the microbiota of *Ido1*^{+/+} and *Ido1*^{-/-} mice using the linear discriminant analysis (LDA) effect size (LefSe) method. When *Ido1*^{+/+} and *Ido1*^{-/-} mice were compared in the unstimulated state (no-DSS) treatment, 11 bacterial taxa were identified as key markers, with increasing numbers of taxa being identified in a dose-dependent manner, 19 taxa in 1% DSS, and 27 taxa in the 2% DSS treatment groups. It is of interest that *Akkermansia*, which has a beneficial role in the mucus layer [27], was enriched in *Ido1*^{-/-} mice only in the 2% DSS treatment group (Fig. 2a). We have previously shown that [15] *Ido1*^{+/+} mice have more severe damage of intestinal barrier integrity compared to *Ido1*^{-/-} mice, when induced by 2% DSS treatment. Moreover, we also confirmed that *Muc1* expression in colon of *Ido1*^{-/-} mice was significantly higher than *Ido1*^{+/+} mice after 2% DSS treatment [15]. These findings support the arguments that

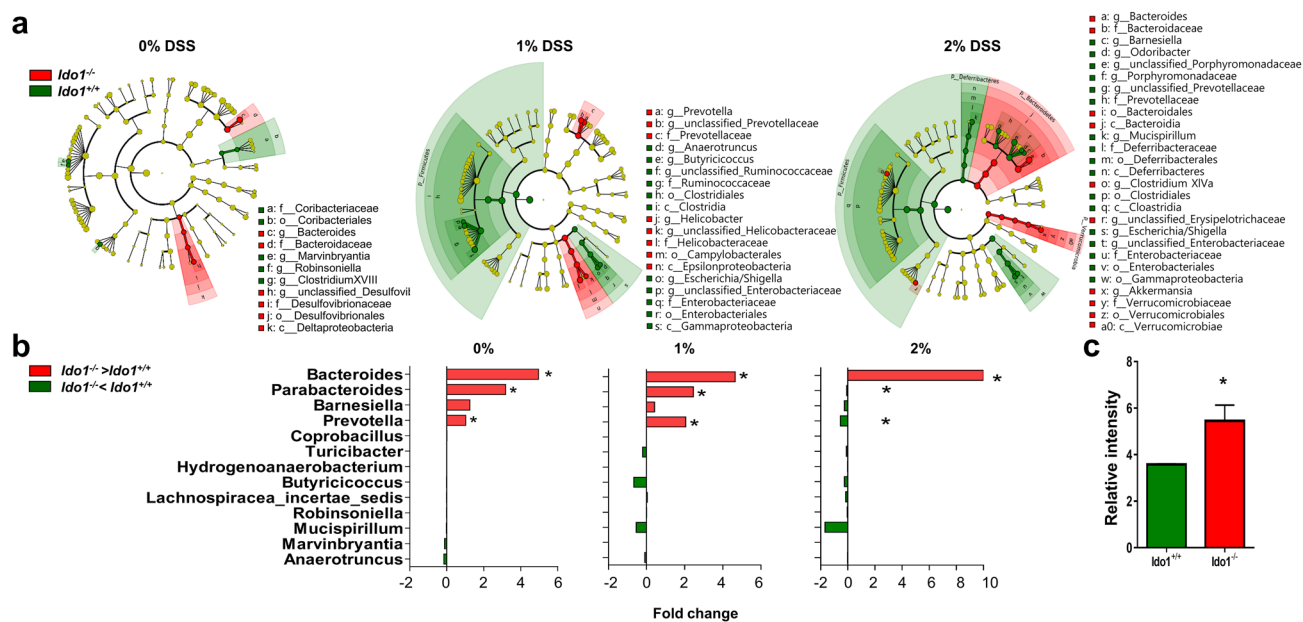


Fig. 2 Comparison of bacterial community composition between *Idol*^{+/+} and *Idol*^{-/-} mice. **a** Taxonomic cladogram from linear discriminant effect size (LEfSe) analysis of gut microbial 16s rRNA sequencing. Only taxa meeting an LDA threshold > 2 and *p* value threshold < 0.1 are shown. **b** Bar graphs summarize the top 13 most differentially detected genera between *Idol*^{+/+} (green) and *Idol*^{-/-}

mice (red) following three doses of DSS. Genera with asterisks are indole-producing bacteria. **c** Comparison of indoxyl sulfate concentration in urine from *Idol*^{+/+} and *Idol*^{-/-} mice. Data are expressed as means ± SEM and analyzed using the two-tailed nonparametric Mann–Whitney *t* test (**p* < 0.05)

the absence of *Ido1* in mice might be attenuate intestinal barrier damage via mucus formation and gut microbial changes. Additionally, this observation supports our previous finding that colitis progression in *Ido*^{-/-} mice was significantly less severe than in *Ido*^{+/+} mice [15]. Because many bacteria in the GI tract can utilize nutrient precursors available in the host lumen [28], we questioned whether the genera that distinguished *Ido*^{-/-} mice from *Ido*^{+/+} mice have metabolic features in common (Fig. 2b). Interestingly, three out of four genera enriched in *Ido*^{-/-} mice, namely *Bacteroides*, *Parabacteroides*, and *Prevotella*, are known to produce an indole-containing compound after utilizing tryptophan [29–31]. This finding that indole-producing bacteria were abundant in the *Ido*^{-/-} mice led us to assume that *Ido*^{-/-} mice contain more indole in the lumen, and therefore absorb, metabolize, and excrete it to a great extent than *Ido*^{+/+} mice. The urinary excretion of 3-indoxyl sulfate, which is a metabolized form of gut bacteria-derived indole by the host [32], was successfully detected by UPLC/Q-TOF-MS/MS. The level of the metabolite was significantly higher in *Idol*^{-/-} mice than in *Idol*^{+/+} mice (Fig. 2c). These findings suggest that the tryptophan, which could not be utilized by the host due to the deficiency in the tryptophan metabolizing enzyme and was left in the GI tract, might be taken up by bacteria that can metabolize tryptophan into indole.

Indole treatment activated transcriptional networks of tight junction integrity in colonic epithelial cell lines in an IDO1-dependent manner

To examine the effect of indole on colon tissues, we treated a colonic epithelial cell line, HCT116, with an indole compound in vitro. Using an Ampli-Seq method, we performed transcriptome analyses of indole-, or vehicle-treated cells that were infected with IDO1-overexpression or empty vectors (Fig. 3a). Although the indole treatment did not change the cell survival (data not shown), it induced substantial changes in the transcriptome (Fig. 3b), resulting in 703 genes identified as DEGs. It was notable that cytoskeleton organization and tight junctions were significantly enhanced at the transcriptional level by indole treatment (Fig. 3c). However, IDO1 overexpression dramatically shut down the beneficial effects of indole on cellular integrity, and even changed the roles of indole to inhibitory, because 36 of 47 components of the tight junction signaling pathway were upregulated in their expression by indole treatment (Fig. 3b) in the cells infected with empty-vector, whereas 29 genes were downregulated in IDO1-overexpressing cells by the same indole treatment (Fig. 3d).

These results implied that commensal bacteria-derived indole might play protective roles in colonic epithelial tight

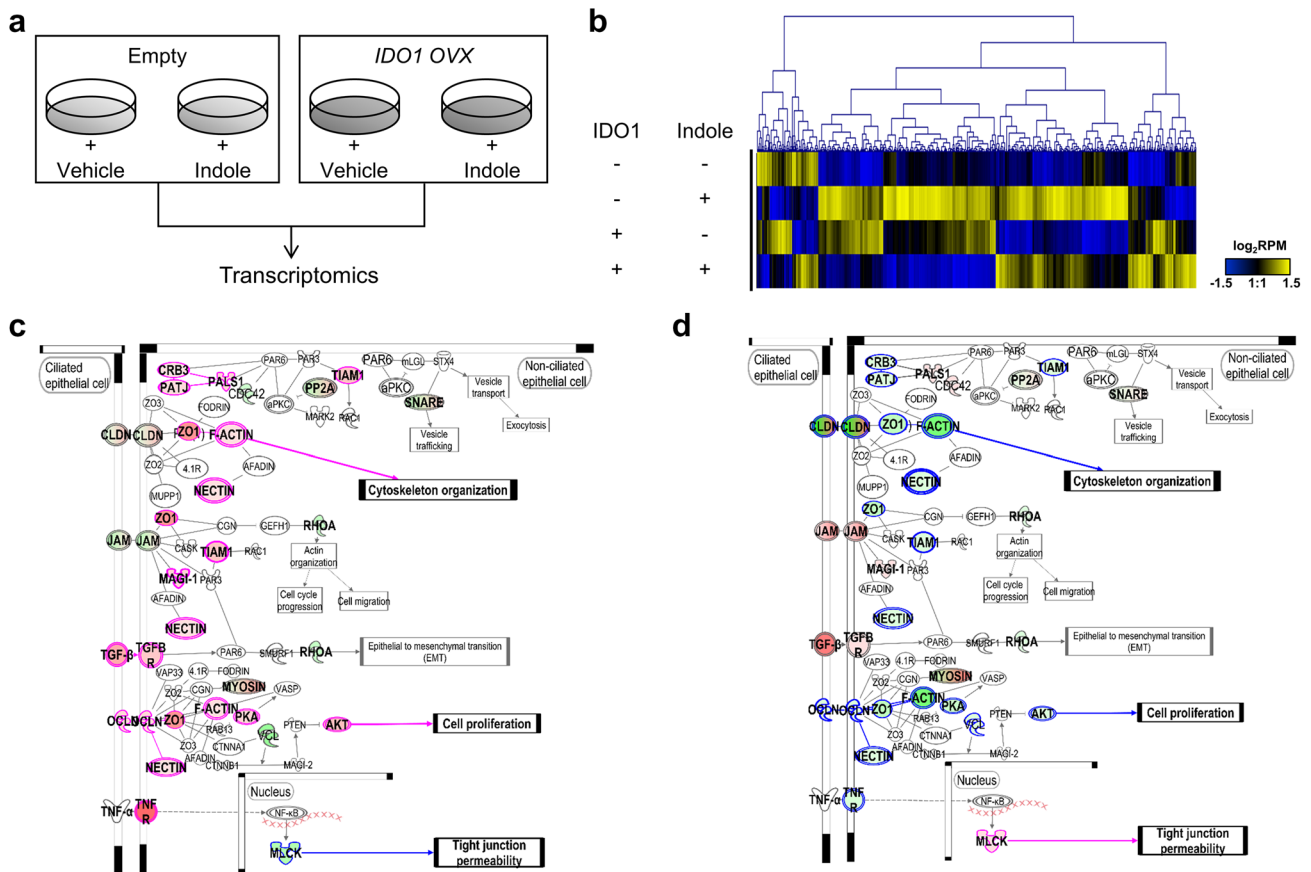


Fig. 3 Treatment of colonic epithelial cell lines with indole in vitro. **a** HCT116 cells infected with IDO1-overexpressing (IDO1 OVX) or empty vector were treated with an indole compound in vitro. Effects of indole treatment on the transcriptome profiles of IDO1 OVX or empty-vector cells were examined by Ampli-Seq technology. **b** Heat map showing hierarchical clustering of 703 DEGs shared between

HCT116 and IDO1-overexpressed HCT116 cells treated with indole. **c, d** Tight junction signaling pathway depicted by ingenuity pathway analysis (IPA). Genes involved in the tight junction pathway that were differently expressed in indole-treated HCT116 (**c**) and IDO1-overexpressed HCT116 cells (**d**). Up- and down- regulated genes are colored in red and green, respectively

junction integrity and the roles were mediated by the levels of IDO1 in the host.

Fecal microbiota transplantation confirmed the interplay between gut microbiota and host tryptophan metabolism

To establish whether the gut microbiota enriched in *Ido1*^{-/-} mice might be transferable and maintain the protective functions against inflammatory injury after transplantation, we carried out an FMT experiment and examined the roles of transplanted microbiota in development of DSS-induced colitis. First, to establish the optimal condition for studying the effect of the gut microbiota during colonic inflammation, we examined the efficiency of the ABX treatment (Fig. 4a). When the C57BL/6 J mice were treated with the ABX regime, and subsequently with DSS treatment, we confirmed that body weight loss and a heightened DAI

were observed only in the no ABX group, while there were no signs of acute colitis in the ABX-treated mice (Fig. 4b, c).

Fresh fecal microbiota from *Ido1*^{-/-} mice were transferred to gut-sterilized *Ido1*^{+/+} mice or *Ido1*^{-/-} mice, and those from *Ido1*^{+/+} mice were transferred to the gut-sterilized *Ido1*^{+/+} mice or *Ido1*^{-/-} mice, after following the ABX regime. During development of DSS-induced colitis, the symptoms of colitis were less severe in the mice colonized with the gut microbiota from *Ido1*^{-/-} mice (both *Ido1*^{+/+} recipient and *Ido1*^{-/-} recipient that harbored *Ido1*^{-/-} microbiota) compared to those mice reconstituted with the gut microbiota from *Ido1*^{+/+} mice (both *Ido1*^{+/+} recipient and *Ido1*^{-/-} recipient that harbored *Ido1*^{+/+} microbiota) (Fig. 4d, e). These data suggest that the gut microbiota of *Ido1*^{-/-} mice played a role in alleviating DSS-induced colitis. On the other hand, in the comparison of two different genotypes that both received the same *Ido1*^{+/+} mice microbiota, *Ido1*^{-/-} recipients showed less severe colitis than *Ido1*^{+/+} recipients. These data showed

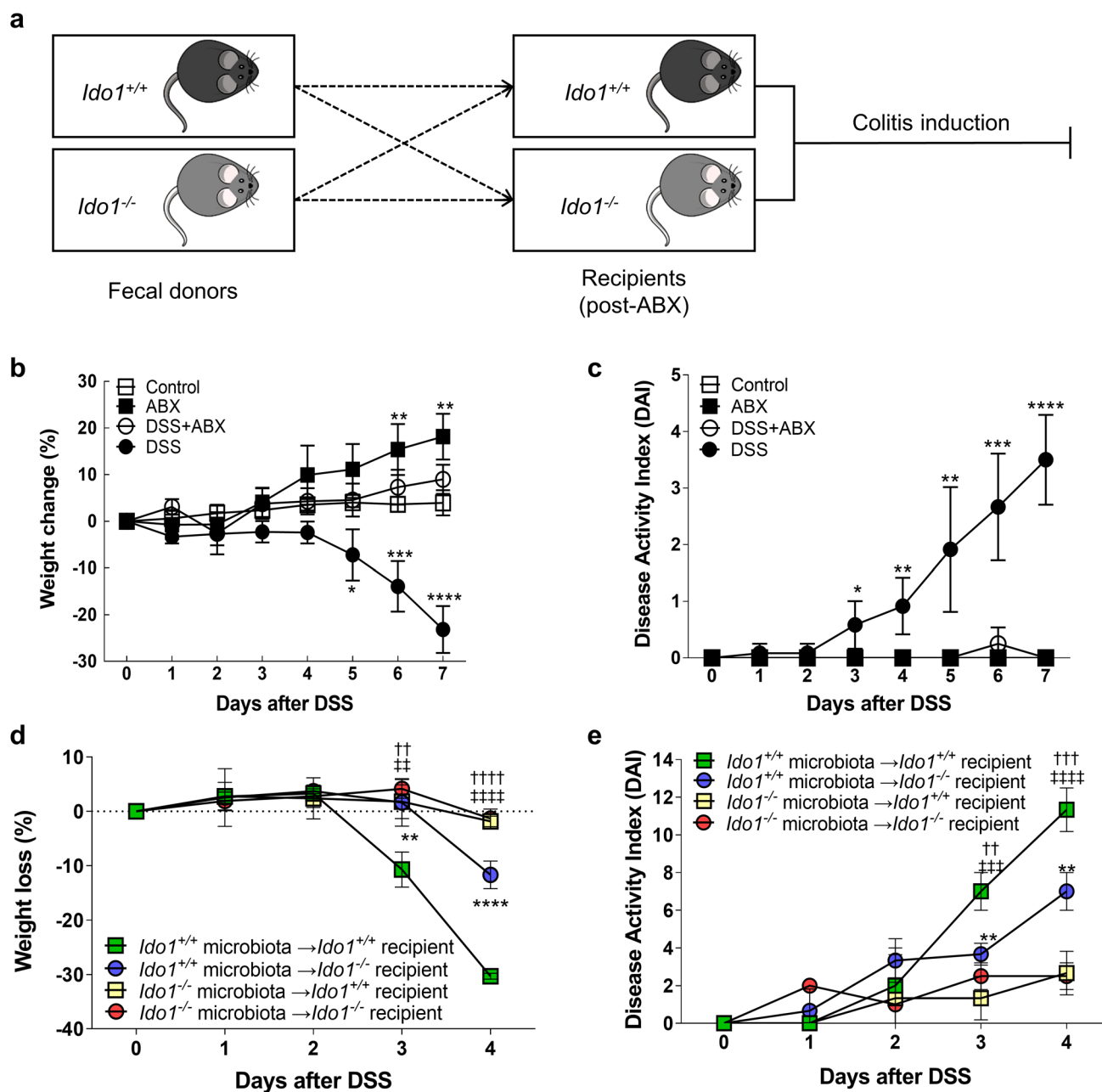


Fig. 4 Effects of transplanted fecal microbiota on the changes in acute colitis development. **a** Healthy C57BL/6J mice were treated with an antibiotic cocktail or not for 4 weeks, and subsequently treated with DSS or no-DSS in drinking water. Disease severity was evaluated by monitoring body weight changes (**b**) and the disease activity index (DAI) (**c**). Asterisks (* $p < 0.05$, ** $p < 0.01$, *** $p < 0.001$, **** $p < 0.0001$) denote body weight changes significantly different from the control, assessed using one-way ANOVA with Bonferroni multiple comparison test. **d**, **e** Fresh fecal micro-

biota from *Ido1*^{-/-} or *Ido1*^{+/+} were transplanted to ABX-treated *Ido1*^{-/-} or *Ido1*^{+/+} mice. After the FMT, recipient mice were stimulated with DSS. Percentage body weight loss (**d**) and DAI (**e**). Values were analyzed by one-way ANOVA followed by Bonferroni multiple comparison test. ** $p < 0.01$; **** $p < 0.0001$. All symbols denote statistical significance compared to the control (*Ido1*^{+/+} → *Ido1*^{+/+}). * Significantly different to *Ido1*^{+/+} → *Ido1*^{-/-}. † Significantly different to *Ido1*^{-/-} → *Ido1*^{+/+}. ‡ Significantly different to *Ido1*^{-/-} → *Ido1*^{-/-}.

that the presence of *Ido1* in the host also contributed to disease severity. Collectively, these findings demonstrated that the effect of gut microbiota composition was more dominant than host genotypes in acute colitis

development and, furthermore provided evidence showing the intercommunication between tryptophan metabolism of the host and the gut microbiota.

Discussion

Dysbiosis of the gut microbiota [33] and nutrient metabolism [34–36] are important factors in the pathogenesis of IBD, but the mechanisms underlying the interconnection between the gut microbiota and host metabolism remain to be elucidated. This study focused on the mechanism by which a lack of host tryptophan catabolism regulates the severity of DSS-induced colitis via alteration of the commensal gut microbiota. Here, we show that *Ido1*-dependent changes in the composition of the intestinal microbiome and their metabolic products exert a protective effect in DSS-treated mice.

Our previous work showed that *Ido1*^{-/-} mice with DSS-mediated colitis experience symptoms that are less severe than those of *Ido1*^{+/+} mice [15]. However, there are other reports that the deficiency or inhibition of *Ido1* exacerbates intestinal inflammation [37, 38]. These discrepancies might result from different experimental settings. In addition to the differences in the pathogenetic mechanism by which TNBS or DSS-induced experimental colitis, it is possible that these inconsistencies might be due to differing compositions of the gut microbiota. In this regard, our data also demonstrated that mice transplanted with the *Ido1*^{-/-} gut microbiota before induction of colitis exhibited an attenuated disease phenotype compared to mice colonized with the *Ido1*^{+/+} microbiota. This substantiates that the gut microbiota is a primary modulator of colitis development in *Ido1*^{-/-} mice.

Various metabolites excreted by commensal bacteria play a crucial role in modulating the physiology of the mammalian intestinal tract. Therefore, another possible mechanism of resistance to DSS-induced colitis is the increased abundance of indole-producing bacteria in *Ido1*^{-/-} mice. Indole is an inter-kingdom signaling molecule that is involved in interactions with the host [29], and is synthesized from tryptophan by the intestinal microbiota [28, 32]. Indole enhanced the expression of proteins involved in the tight junction signaling pathway in colon cancer cell lines, which is in agreement with other studies [39, 40]. Intestinal barrier dysfunction, which is observed in both IBD patients and experimental colitis models, may exacerbate IBD susceptibility [41, 42]. Zelate et al. [43] showed that, in *Ido1*-deficient mice, *Lactobacilli* convert tryptophan to indole-3-aldehyde (IAld), which protects against *Candida albicans* colonization. We assume that indole derivatives produced by the gut microbiota of *Ido1*^{-/-} mice not only influence intestinal barrier integrity but also disrupt colonization by pathogenic bacteria [44, 45].

Recently, host–gut microbiota interactions, which directly or indirectly contribute to host physiology, have

been the focus of several studies. Nutrition is a particularly important factor in this interaction. We found that the cause of disease is different, based on the changes in gut microbiota caused by tryptophan metabolic deficiency of the host. This supports the notion that disease progression is influenced by tryptophan metabolism by both the gut microbiota and the host. In parallel, the lack of the *Ace2* gene, which is related to tryptophan absorption, in mice with DSS-induced colitis resulted in a significant difference in the severity of intestinal inflammation compared to control mice [46]. However, many questions about host–gut microbiota interactions in IBD remain unanswered. Hence, future studies should investigate other systemic communications with gut microbiota, and not be confined to the gastrointestinal tract.

To our knowledge, this study is the first to analyze the profiling of gut microbiota in *Ido1*^{-/-} mice. We demonstrated that altered gut microbiota in *Ido1*^{-/-} mice ameliorates the symptoms of DSS-induced colitis. Due to the inability of *Ido1*^{-/-} mice to metabolize tryptophan, it might be relatively abundant in the large intestine, resulting in increased abundance of microbial genera that metabolize tryptophan to indole-containing compounds. The contribution of bacteria-derived indole to intestinal barrier integrity depended on the down-regulation of *Ido1* expression. However, this study has a limitation that the relationship between the gut microbiota and intestinal inflammation has been confirmed using only genetic defect models of tryptophan metabolism. Thus, further research is needed to investigate the direct effect of a tryptophan-deficient/rich diet on gut inflammation. Additionally, our findings provide further evidence that the host communicates with its commensal gut microbiota by means of shared tryptophan metabolism networks. Although further research is required to validate our findings that indole and the indole-producing bacteria can predict IBD risk, increased knowledge of the role of the gut microbiota and its metabolite, indole, might lead to development of more effective therapeutic options for IBD. Moreover, our findings suggested that reciprocal interactions between the gut microbiota and the host inflammatory response may be mediated by shared tryptophan metabolism networks.

Acknowledgements This research was supported by the Seoul National University Research Grant.

Author contributions This study was designed, directed, and coordinated by D-MS, EYC, and J-HS. HCM, D-MS, and EYC supervised the project. J-HS, W-JS, and Y-KL acquired data and performed the animal experiments. Detection of metabolites in urine was analyzed by BK and J-YC. J-HS analyzed and interpreted data. JHS and DMS wrote the main paper, and Y-KL and BK wrote the Materials and Methods section. COJ gave technical and material support. All authors discussed the results and implications and commented on the manuscript at all stages.

Compliance with ethical standards

Conflict of interest The authors declare that they have no conflict of interest.

Ethical approval The protocol of this study was approved by the Institutional Animal Care and Use Committee of the Institute of Laboratory Animal Resources, Seoul National University (Institutional Animal Care and Use Committee permit number: SNU-150119-5).

References

- O'Hara AM, Shanahan F (2006) The gut flora as a forgotten organ. *EMBO Rep* 7(7):688–693
- Sartor RB (2008) Microbial influences in inflammatory bowel diseases. *Gastroenterology* 134(2):577–594
- Scott KP, Gratz SW, Sheridan PO, Flint HJ, Duncan SH (2013) The influence of diet on the gut microbiota. *Pharmacol Res* 69(1):52–60
- Hesla HM, Stenius F, Jäderlund L, Nelson R, Engstrand L, Alm J, Dicksved J (2014) Impact of lifestyle on the gut microbiota of healthy infants and their mothers—the ALADDIN birth cohort. *FEMS Microbiol Ecol* 90(3):791–801
- Shin J-H, Sim M, Lee J-Y, Shin D-M (2016) Lifestyle and geographic insights into the distinct gut microbiota in elderly women from two different geographic locations. *J Physiol Anthropol* 35(1):31–39
- Yatsunenko T, Rey FE, Manary MJ, Trehan I, Dominguez-Bello MG, Contreras M, Magris M, Hidalgo G, Baldassano RN, Anokhin AP, Heath AC, Warner B, Reeder J, Kuczynski J, Caporaso JG, Lozupone CA, Lauber C, Clemente JC, Knights D, Knight R, Gordon JI (2012) Human gut microbiome viewed across age and geography. *Nature* 486(7402):222–227
- Grzeskowiak L, Collado MC, Mangani C, Maleta K, Laitinen K, Ashorn P, Isolauri E, Salminen S (2012) Distinct gut microbiota in southeastern African and northern European infants. *J Pediatr Gastroenterol Nutr* 54(6):812–816
- Dehingia M, Talukdar NC, Talukdar R, Reddy N, Mande SS, Deka M, Khan MR (2015) Gut bacterial diversity of the tribes of India and comparison with the worldwide data. *Sci Rep* 5:18563
- Senghor B, Sokhna C, Ruimy R, Lagier J-C (2018) Gut microbiota diversity according to dietary habits and geographical provenance. *Hum Microbiome J* 7:1–9
- Bassett SA, Young W, Barnett MP, Cookson AL, McNabb WC, Roy NC (2015) Changes in composition of caecal microbiota associated with increased colon inflammation in interleukin-10 gene-deficient mice inoculated with enterococcus species. *Nutrients* 7(3):1798–1816
- Gálvez EJ, Iljazovic A, Gronow A, Flavell R, Strowig T (2017) Shaping of intestinal microbiota in Nlrp6- and Rag2-deficient mice depends on community structure. *Cell Rep* 21(13):3914–3926
- Kim CJ, Kovacs-Nolan JA, Yang CB, Archbold T, Fan MZ, Mine Y (2010) L-Tryptophan exhibits therapeutic function in a porcine model of dextran sodium sulfate (DSS)-induced colitis. *J Nutr Biochem* 21(6):468–475
- Shizuma T, Mori H, Fukuyama N (2013) Protective effect of tryptophan against dextran sulfate sodium-induced experimental colitis. *Turk J Gastroenterol* 24(1):30–35
- Ciorba MA (2013) Indoleamine 2, 3 dioxygenase (IDO) in intestinal disease. *Curr Opin Gastroenterol* 29(2):146
- Shon W-J, Lee Y-K, Shin JH, Choi EY, Shin D-M (2015) Severity of DSS-induced colitis is reduced in Idol1-deficient mice with down-regulation of TLR-MyD88-NF-kB transcriptional networks. *Sci Rep* 5:17305
- Cole JR, Wang Q, Fish JA, Chai B, McGarrell DM, Sun Y, Brown CT, Porras-Alfaro A, Kuske CR, Tiedje JM (2014) Ribosomal Database Project: data and tools for high throughput rRNA analysis. *Nucleic Acids Res* 42(Database issue):D633–642
- Edgar RC, Haas BJ, Clemente JC, Quince C, Knight R (2011) UCHIME improves sensitivity and speed of chimera detection. *Bioinformatics* 27(16):2194–2200
- Wang GGM, Tiedje JM, Cole JR (2007) Naive Bayesian classifier for rapid assignment of rRNA sequences into the new bacterial taxonomy. *Appl Environ Microbiol* 73(16):5261–5267
- Lee Y-K, Lee HB, Shin D-M, Kang MJ, Yi EC, Noh S, Lee J, Lee C, Min C-K, Choi EY (2014) Heme-binding-mediated negative regulation of the tryptophan metabolic enzyme indoleamine 2, 3-dioxygenase 1 (IDO1) by IDO2. *Exp Mol Med* 46(11):e121
- Zhang JD, Schindler T, Kung E, Ebeling M, Certa U (2014) Highly sensitive amplicon-based transcript quantification by semiconductor sequencing. *BMC Genom* 15:565
- Li Z, Huang J, Zhao J, Chen C, Wang H, Ding H, Wang DW, Wang DW (2014) Rapid molecular genetic diagnosis of hypertrophic cardiomyopathy by semiconductor sequencing. *J Transl Med* 12:173
- Hartley JW, Chattopadhyay SK, Lander MR, Taddesse-Heath L, Naghashfar Z, Morse HC 3rd, Fredrickson TN (2000) Accelerated appearance of multiple B cell lymphoma types in NFS/N mice congenic for ecotropic murine leukemia viruses. *Lab Invest* 80(2):159–169
- Wu H-J, Ivanov II, Darce J, Hattori K, Shima T, Umesaki Y, Littman DR, Benoist C, Mathis D (2010) Gut-residing segmented filamentous bacteria drive autoimmune arthritis via T helper 17 cells. *Immunity* 32(6):815–827
- Karmarkar D, Rock KL (2013) Microbiota signalling through MyD88 is necessary for a systemic neutrophilic inflammatory response. *Immunology* 140(4):483–492
- Reikvam DH, Erofeev A, Sandvik A, Grcic V, Jahnsen FL, Gaustad P, McCoy KD, Macpherson AJ, Meza-Zepeda LA, Johansen F-E (2011) Depletion of murine intestinal microbiota: effects on gut mucosa and epithelial gene expression. *PLoS ONE* 6(3):e17996
- Segata N, Izard J, Waldron L, Gevers D, Miropolsky L, Garrett WS, Huttenhower C (2011) Metagenomic biomarker discovery and explanation. *Genome Biol* 12(6):R60
- Reunanen J, Kainulainen V, Huuskonen L, Ottman N, Belzer C, Huhtinen H, de Vos WM, Satokari R (2015) *Akkermansia muciniphila* adheres to enterocytes and strengthens the integrity of epithelial cell layer. *Appl Environ Microbiol* 81(11):3655–3662
- Sridharan GV, Choi K, Klemashevich C, Wu C, Prabakaran D, Pan LB, Steinmeyer S, Mueller C, Yousofshahi M, Alaniz RC (2014) Prediction and quantification of bioactive microbiota metabolites in the mouse gut. *Nat Commun* 5:5492
- Lee J-H, Lee J (2010) Indole as an intercellular signal in microbial communities. *FEMS Microbiol Rev* 34(4):426–444
- Yokoyama M, Carlson J (1979) Microbial metabolites of tryptophan in the intestinal tract with special reference to skatole. *Am J Clin Nutr* 32(1):173–178
- Russell WR, Duncan SH, Scobbie L, Duncan G, Cantlay L, Calder AG, Anderson SE, Flint HJ (2013) Major phenylpropanoid-derived metabolites in the human gut can arise from microbial fermentation of protein. *Mol Nutr Food Res* 57(3):523–535
- Wikoff WR, Anfora AT, Liu J, Schultz PG, Lesley SA, Peters EC, Siuzdak G (2009) Metabolomics analysis reveals large effects of gut microflora on mammalian blood metabolites. *Proc Natl Acad Sci USA* 106(10):3698–3703

33. Sokol H, Lay C, Seksik P, Tannock GW (2008) Analysis of bacterial bowel communities of IBD patients: what has it revealed? *Inflamm Bowel Dis* 14(6):858–867
34. Gupta NK, Thaker AI, Kanuri N, Riehl TE, Rowley CW, Stenson WF, Ciorba MA (2012) Serum analysis of tryptophan catabolism pathway: correlation with Crohn's disease activity. *Inflamm Bowel Dis* 18(7):1214–1220
35. Sun J (2018) Dietary vitamin D, vitamin D receptor, and microbiome. *Curr Opin Clin Nutr Metab Care* 21(6):471
36. Ghazalpour A, Cespedes I, Bennett BJ, Allayee H (2016) Expanding role of gut microbiota in lipid metabolism. *Curr Opin Lipidol* 27(2):141–147
37. Gurtner GJ, Newberry RD, Schloemann SR, McDonald KG, Stenson WF (2003) Inhibition of indoleamine 2,3-dioxygenase augments trinitrobenzene sulfonic acid colitis in mice. *Gastroenterology* 125(6):1762–1773
38. Takamatsu M, Hirata A, Ohtaki H, Hoshi M, Hatano Y, Tomita H, Kuno T, Saito K, Hara A (2013) IDO1 plays an immunosuppressive role in 2, 4, 6-trinitrobenzene sulfate-induced colitis in mice. *J Immunol* 191(6):3057–3064
39. Shimada Y, Kinoshita M, Harada K, Mizutani M, Masahata K, Kayama H, Takeda K (2013) Commensal bacteria-dependent indole production enhances epithelial barrier function in the colon. *PLoS ONE* 8(11):e80604
40. Bansal T, Alaniz RC, Wood TK, Jayaraman A (2010) The bacterial signal indole increases epithelial-cell tight-junction resistance and attenuates indicators of inflammation. *Proc Natl Acad Sci USA* 107(1):228–233
41. Poritz LS, Garver KI, Green C, Fitzpatrick L, Ruggiero F, Koltun WA (2007) Loss of the tight junction protein ZO-1 in dextran sulfate sodium induced colitis. *J Surg Res* 140(1):12–19
42. Mankertz J, Schulzke JD (2007) Altered permeability in inflammatory bowel disease: pathophysiology and clinical implications. *Curr Opin Gastroenterol* 23(4):379–383
43. Zelante T, Iannitti RG, Cunha C, De Luca A, Giovannini G, Pieraccini G, Zecchi R, D'Angelo C, Massi-Benedetti C, Fallarino F, Carvalho A, Puccetti P, Romani L (2013) Tryptophan catabolites from microbiota engage aryl hydrocarbon receptor and balance mucosal reactivity via interleukin-22. *Immunity* 39(2):372–385
44. Oh S, Go GW, Mylonakis E, Kim Y (2012) The bacterial signaling molecule indole attenuates the virulence of the fungal pathogen *Candida albicans*. *J Appl Microbiol* 113(3):622–628
45. Lee JH, Cho HS, Kim Y, Kim JA, Banskota S, Cho MH, Lee J (2013) Indole and 7-benzyloxyindole attenuate the virulence of *Staphylococcus aureus*. *Appl Microbiol Biotechnol* 97(10):4543–4552
46. Hashimoto T, Perlot T, Rehman A, Trichereau J, Ishiguro H, Paolino M, Sigl V, Hanada T, Hanada R, Lipinski S, Wild B, Camargo SM, Singer D, Richter A, Kuba K, Fukamizu A, Schreiber S, Clevers H, Verrey F, Rosenstiel P, Penninger JM (2012) ACE2 links amino acid malnutrition to microbial ecology and intestinal inflammation. *Nature* 487(7408):477–481